Mutational Analysis of Potential Zinc-Binding Residues in the Active Site of the Enterococcal D-Ala-D-Ala Dipeptidase VanX†

Dewey G. McCafferty,‡ Ivan A. D. Lessard,‡ and Christopher T. Walsh*

Department of Biological Chemistry and Molecular Pharmacology, Harvard Medical School, Boston, Massachusetts 02115

Received March 10, 1997; Revised Manuscript Received June 4, 1997⊗

ABSTRACT: VanX, one of the five proteins required for the vancomycin-resistant phenotype in clinically pathogenic *Enterococci*, is a zinc-containing D-Ala-D-Ala dipeptidase. To identify potential zinc ligands and begin defining the active site residues, we have mutated the 2 cysteine, 5 histidine, and 4 of the 28 aspartate and glutamate residues in the 202 residue VanX protein. Of 10 mutations, 3 cause inactivation and greater than 90% loss of zinc in purified enzyme samples, implicating His116, Asp123, and His184 as zinc-coordinating residues. Homology searches using the 10 amino acid sequence SxHxxGxAxD, in which histidine and aspartate residues are putative zinc ligands, identified the metal coordinating ligands in the N-terminal domain of the murine Sonic hedgehog protein, which also exhibits an architecture for metal coordination identical to that observed in thermolysin from *Bacillus thermoproteolyticus*. Furthermore, this 10 amino acid consensus sequence is found in the *Streptomyces albus* G zinc-dependent *N*-acyl-D-Ala-D-Ala carboxypeptidase, an enzyme catalyzing essentially the same D-Ala-D-Ala dipeptide bond cleavage as VanX, suggesting equivalent mechanisms and zinc catalytic site architectures. VanX residue Glu181 is analogous to the Glu143 catalytic base in *B. thermoproteolyticus* thermolysin, and the E181A VanX mutant has no detectable dipeptidase activity, yet maintains near-stoichiometric zinc content, a result consistent with the participation of the residue as a catalytic base.

The development of clinically significant resistance to the glycopeptide antibiotic vancomycin has been shown to require the expression of five vancomycin-resistance genes, *vanS, -R, -H, -A,* and *-X* (Arthur *et al.*, 1993). Homology analyses of the predicted open reading frames encoded by *vanS, -R, -H,* and *-A* have allowed us to identify a putative role for each protein, to devise assays, and, upon purification of each of these four proteins, to test for specific catalytic activities. The prediction that VanS and VanR comprise a two-component sensor/response regulator system with phospho-VanR as the transcriptional activator of the *vanHAX* operon was subsequently validated (Wright *et al.*, 1993). VanH was also determined to be a D-lactate dehydrogenase that reduced pyruvate to D-lactate (Bugg *et al.*, 1991b), and the D-lactate could be used by VanA in conjunction with ATP and D-Ala to make a D-Ala-D-lactate depsipeptide (Bugg *et al.*, 1991a). This depsipeptide ligase activity is a gain of function modification in VanA compared to the homologous D-Ala-D-Ala ligases (Ddls), which could synthesize the D-Ala-D-Ala dipeptide but not the depsipeptide. Subsequently, Ddl from the vancomycin-resistant organism *Leuconostoc mesenteroides* has been found to synthesize D-Ala-D-lactate (Park & Walsh, 1997). Consequently, the cell wall in the naturally resistant Gram-positive bacteria (*Leuconostoc*, *Lactobacillus*, *Pediococcus*, etc.) and in the vancomycin-resistant enterococcal clinical pathogens utilizes peptidoglycan intermediates terminating in D-Ala-D-lactate rather than D-Ala-D-Ala (Handwerger *et al.*, 1994; Billot-Klein *et al.*, 1994), thereby accounting for a 10^3-10^4-fold lower affinity for vancomycin (Bugg *et al.*, 1991a).

The function of the fifth required gene, *vanX*, was not decipherable from DNA sequence homologies until the observation of D-Ala-D-Ala dipeptidase activity in crude extracts of VanX-expressing cells (Reynolds *et al.*, 1994). Purification to homogeneity of overproduced VanX in *Escherichia coli* led to the demonstration that VanX is a zinc-dependent dipeptidase specific for D-,D-dipeptides with a 10^6-fold selectivity in k_{cat}/K_M for hydrolyzing D-Ala-D-Ala versus D-Ala-D-lactate (Wu *et al.*, 1995). Thus, in *Enterococcus* expressing VanX, D-Ala-D-lactate accumulates, while competing D-Ala-D-Ala is hydrolyzed back to D-Ala monomers. Only D-Ala-D-lactate is available as a substrate for the subsequent enzyme, MurF, to yield uridine diphosphate *N*-acetylmuramic acid−tetrapeptide−D-lactate, thereby accounting for quantitative resistance to vancomycin (Walsh *et al.*, 1996).

Initial searches for homology of the 202 amino acid VanX to other zinc-dependent proteases and peptidases failed to detect consensus catalytic zinc binding motifs (e.g., HEXXH for thermolysin; Vallee & Auld, 1990). We have instead pursued a mutagenesis strategy directed at the histidine, glutamate, and aspartate residues in VanX, and report herein the identification of three putative metal binding residues and a residue which may function as a catalytic base. Furthermore, homology of this putative zinc coordination site to the N-terminal domain of murine Sonic hedgehog (Shh-N; Tanaka-Hall *et al.*, 1995)[1] and, intriguingly, to the zinc-dependent *N*-acyl-D-Ala-D-Ala carboxypeptidase of *Streptomyces albus* G (Ddp; Dideberg *et al.*, 1982) is revealed.

† This research was supported by NIH Grant GM 49338 to C.T.W. I.A.D.L. received postdoctoral fellowship support from the Natural Sciences and Engineering Research Council of Canada.

* Corresponding author. Phone: 617-432-1715. FAX: 617-432-0556. E-mail: walsh@walsh.med.harvard.edu.

‡ D.G.M. and I.A.D.L. contributed equally to this work.

⊗ Abstract published in *Advance ACS Abstracts,* August 1, 1997.

S0006-2960(97)00543-6 CCC: $14.00

EXPERIMENTAL PROCEDURES

Materials. Bacteriological media were obtained from Difco Laboratories. The prokaryotic expression vector pET28b(+), competent *E. coli* strain BL21(DE3) [F-, *ompT*, *hsdS*$_B$, (r_{B^-},m_{B^-}), *gal*, *dcm*, (DE3)], and restriction-grade thrombin were purchased from Novagen. Competent *E. coli* strain DH5α [F^-, ϕ80d*lac*ZΔM15, Δ(*lac*ZYA-*arg*F)U169, *deo*R, *rec*A1, *end*A1, *hsd*R17(r_K^-, m_K^+), *pho*A, *sup*E44, λ^-, *thi*-1, *gyr*A96, *rel*A1] was purchased from GibcoBRL. Restriction endonucleases, T4 DNA ligase, calf intestinal alkaline phosphatase (CIAP), prokaryotic expression vector pMAL-c2, and amylose resin were obtained from New England Biolabs. *Pfu* DNA polymerase was purchased from Stratagene. Isopropyl 1-thio-β-D-galactopyranoside (IPTG) was purchased from Bachem Biosciences. (+)-D-10-Camphorsulfonic acid, ampicillin, and kanamycin were purchased from Sigma. Chelex-100 resin and low molecular weight markers for polyacrylamide gel electrophoresis (PAGE) were obtained from Bio-Rad. Plasmid pZW011 expressing the *vanX* gene from type A vancomycin-resistant *Enterococci* has been described previously (Wu & Walsh, 1995).

Recombinant DNA Methods. Recombinant DNA techniques were performed as described elsewhere (Sambrook *et al.*, 1989). Preparation of plasmid DNA, gel purification of DNA fragments, and purification of polymerase chain reaction (PCR) amplified DNA fragments (Saiki *et al.*, 1985, 1988) were performed using a QIAprep spin plasmid miniprep kit, a QIAEX II gel extraction kit, and a QIAquick PCR purification kit, respectively (QIAGEN). PCRs were carried out as described by Lessard and Perham (1994), using the *pfu* DNA polymerase. Splicing by overlap extension (SOE) reactions (Ho *et al.*, 1989) were carried out as for the PCR using approximately an equimolar ratio (total amount ca. 50 ng) of each of the gel-purified PCR-amplified DNA fragments to be joined as template. The fidelity of the SOE- or PCR-amplified DNA fragments was established by nucleotide sequencing after subcloning into the expression vector. Oligonucleotide primers were obtained from Integrated DNA Technologies, and DNA sequencing was performed on double-stranded DNA by the Molecular Biology Core Facility of the Dana Farber Cancer Institute (Boston, MA).

Construction of Expression Vector for MBP−VanX Fusion Proteins. The expression vector for maltose binding protein−VanX (MBP−VanX) fusion protein (pIADL14) was constructed from a pET28b(+) plasmid template. The genes encoding MBP (*malE*) and VanX (*vanX*) were obtained from plasmids pMAL-c2 and pZW011, respectively. The primers used for all PCR and SOE mutagenesis are depicted in Table 1. Prior to pIADL14 construction, two modifications of the *malE* gene were made. First, the 5′-terminal codon of the *malE* gene corresponding to Ser2 was mutated by PCR to code for a glycine residue, in order to introduce a *Nco*I restriction site for cloning and to position the starting codon at the proper distance from the ribosome binding site. Second, the internal *Nco*I site of the *malE* gene was removed by silent mutagenesis using the SOE method.

Table 1: Oligonucleotide Primers for Site-Directed Mutagenesis[a]

Comment	Code	5′-3′ Nucleotide Sequence
MBP$_{NcoI\ Removal}$	1012	GGCGTTTTCCATT**G**TGGCGGCAATACGTGG
MBP$_{NcoI\ Removal}$	2012	CGTATTGCCGCCAC**A**ATGGAAAACGCCC
MBP$_{NcoI}$	2011	**G**G**GC**CATG**G**GAATCGAAGAAGGTAAACTGG
MBP$_{Thrombin}$	1015	**CG**TG**G**AA**C**C**AG**TCC**GCT**G**C**TCCCGAGGTTGTTGTTATTGTTA
MBP$_{NdeI}$	1014	**CCTATTTCCATATGGGATCCT**CGTGGAACCAGTCCGCTGCTC-CCGAGG
T7$_{prom}$	2001	ACTGTTTTATGCAATGGGCTGC
T7$_{term}$	1001	CAGCCAACTCAGCTTCCTTTCG
VanX$_{Internal}$	2002	GGGAATTGTGAGCGGATAACA
H13A	21DI	GAGATATACATATGGAAATAGGATTTACTTTTTTAGATGAAATAG-TA**GC**CGGTGTTCG
H116A	1108	GGCACTGCCGCGGCTA**GC**GCTTGATTTTGAAGC
D123A	2108	AGCCATAGCCGCGGCAGTGCCATTG**C**TCTTACGCTTTATCG
D145A	2101	TTTATGG**C**TGAACGCTCTCATC
D145A	1101	AGAGCGTTCA**G**CCATAAAATCAAATC
E146A	2102	ATGGATG**C**ACGCTCTCATCATGC
E146A	1102	ATGAGAGCGT**G**CATCCATAAAATC
D145A/E146A	2112	ATGG**C**TG**C**ACGCTCTCATCATGC
D145A/E146A	1112	ATGAGAGCGT**G**CA**G**CCATAAAATC
H149A	2103	ACGCTCT**GC**TCATGCGGCAAATGG
H149A	1103	GCCGCATGA**GC**AGAGCGTTCATC
H150A	2104	ACGCTCTCAT**GC**TGCGGCAAATGG
H150A	1104	GCCGCA**GC**ATGAGAGCGTTCATC
H149A/H150A	2113	ACGCTCT**GC**TGCTGCGGCAAATGGA
H149A/H150A	1113	GCCGCAGCA**GC**AGAGCGTTCATC
E181A	2115	TATAGCCTCG**CC**TGGTGGCACTATGT
E181A	1115	AGTGCCACCA**GG**CGAGCCTATATG
H184A	2111	CGAATGGTGG**GC**CTATGTATTAAGAG
H184A	1111	CTTAATACATAG**GC**CCACCATTCGAGG
C78S	2105	CTGTAAACT**C**TTTTATGCAATGGG
C78S	1107	GCCCATTGCATAAAA**G**AGTTTACAGCACGC
C157S	2107	GCAAATGGAATATCAT**C**CAATGAAGCGCAA
C157S	1106	GCTTCATTG**G**ATGATATTCCAT

[a] Mismatch mutations are underlined and in boldface.

For the first round of PCR, the sequences upstream and downstream of the internal *Nco*I site were separately amplified from pMAL-c2 using the sense/antisense primer pairs 2011/1012 and 2012/1015, respectively (Table 1). The resulting DNA fragments were gel-purified and subjected to a second round of PCR using the primer pair 2011/1014. At the C-terminal sequence, the serine/arginine-rich linker originally designed for pMAL-c2 was extended by the introduction of a thrombin cleavage site (LVPRGS) followed by a His-Met sequence encoded by an *Nde*I restriction site. The purified SOE-amplified DNA fragment was then digested with *Nde*I and *Nco*I, gel-purified, and subcloned into pET28b(+) digested with *Nde*I and *Nco*I and treated with CIAP, to create plasmid pIADL16. Plasmid pZW011 was digested with *Nde*I and *Hin*dIII, and the resulting *vanX*-containing DNA fragment was gel-purified and subcloned into pIADL16 digested with *Nde*I and *Hin*dIII and treated with CIAP. The resulting plasmid (pIADL14) encodes an MBP−VanX fusion protein with a serine/arginine-rich linker followed by a thrombin cleavage site (Figure 1). Thrombin proteolysis of the MBP−VanX fusion protein leaves the N-terminal tripeptide sequence Gly-Ser-His at positions −3 to −1 prior to the starting methionine of VanX.

Site-Directed Mutagenesis. Site-directed mutants D123A, H116A, and H13A were constructed from a pZW011 template by PCR mutagenesis using the sense/antisense primer pairs 2108/1001, 1108/2002, and 21DI/1001, respectively. The purified PCR-amplified DNA fragments were digested with *Sac*II and *Hin*dIII for the D123A mutant and with *Nde*I and *Sac*II for the H116A and H13A mutants, gel-purified, and subcloned into a pIADL14 plasmid backbone digested with the appropriate restriction endonucleases and treated with CIAP. Site-directed mutants D145A, E146A, H149A, H150A, E181A, H184A, D145A/E146A, and H149A/H150A were constructed using the SOE method. In the first

[1] Abbreviations: CD, circular dichroism; CIAP, calf intestinal alkaline phosphatase; D-Ala, D-alanine; D-Ala-D-Ala, D-alanyl-D-alanyl dipeptide; D-Ala-D-lactate, D-alanyl-D-lactate depsipeptide; Ddp, *N*-acyl-D-Ala-D-Ala carboxypeptidase; IPTG, isopropyl 1-thio-β-D-galactoside; LB, Luria broth; MBP, maltose-binding protein; PCR, polymerase chain reaction; PAGE, polyacrylamide gel electrophoresis; Shh-N, Sonic hedgehog protein N-terminal fragment; SOE, splicing by overlap extension.

round of PCR, the sequence upstream and downstream of the mutation was amplified separately using a pZW011 plasmid template and the sense/antisense primer pairs 2001/11XX and 21XX/1001, respectively (Table 1, each mutant corresponds to a particular XX pair of primers). The resulting PCR-amplified DNA fragments were gel-purified and subjected to a second round of PCR using the 2002/1001 primer pair. The purified SOE-amplified DNA fragment was digested with *Sac*II and *Hin*dIII, gel-purified, and subcloned into the *Sac*II- and *Hin*dIII-digested/CIAP-treated pIADL14. The H116A/H184A double mutant was constructed from the parent single mutant plasmids (pIADL14-H116A and pIADL14-H184A) by digesting pIADL14-H116A with *Nde*I and *Sac*II, gel-purifying the 5′-end *vanX*-containing DNA fragment, and subcloning into the *Nde*I- and *Sac*II-digested/CIAP-treated pIADL14-H184A plasmid. The C78S/C157S double mutant was constructed from three separate amplified DNA fragments using SOE. In the first round of PCR, three DNA fragments were separately amplified using a pZW011 plasmid template and the primer pairs 2002/1107, 2105/1106, and 2107/1001. The resulting three PCR-amplified DNA fragments were gel-purified and subjected to a second round of PCR using the 2002/1001 primer pair. The resulting purified SOE-amplified DNA fragment was subsequently digested with *Nde*I and *Hin*dIII, gel-purified, and subcloned into the *Nde*I- and *Hin*dIII-digested/CIAP-treated pIADL14 plasmid.

Overexpression of the Gene Encoding MBP−VanX Fusion. One colony of freshly transformed *E. coli* strain BL21-(DE3) was dispersed in 200 μL of Luria broth (LB) medium by vortexing, plated onto a kanamycin (50 μg/mL) LB medium agar plate (100 × 15 mm), and grown overnight at 37 °C. The lawn of cells was resuspended in LB medium (3 mL) and used to inoculate 1 L of LB medium supplemented with 200 μM $ZnSO_4$ and 50 μg/mL kanamycin. The inoculum was grown at 30 °C to an OD_{600} of 1.8, at which point IPTG was added to a final concentration of 1 mM. After 75 min of induction at 30 °C, the cells were harvested by centrifugation and used immediately or stored at −80 °C.

Purification of MBP−VanX. All steps were performed at 4 °C unless otherwise noted. Cell pellets from 1 L of culture were resuspended (2 mL/g of wet cells) in buffer A (20 mM Tris-HCl, pH 7.6/200 mM NaCl) and disrupted twice in a French pressure cell (18 000 psi). Cellular debris was removed by centrifugation (95000*g*, 20 min), and the supernatant collected was diluted to 50 mL with buffer A. The supernatant was applied to an amylose column (150 × 26 mm, 0.5 mL/min flow rate) previously equilibrated with buffer A and washed with 160 mL of buffer A (flow rate increased to 1 mL/min), and the desired MBP−VanX fusion protein was eluted with buffer B (20 mM Tris-HCl, pH 7.6/10 mM maltose/200 mM NaCl). Fractions (5 mL each) containing the recombinant MBP−VanX fusion protein were analyzed for purity by SDS−PAGE with the pure fractions pooled and dialyzed for two changes, 4 h each, against 2 L of buffer C (20 mM Tris-HCl, pH 8.4/150 mM NaCl). After dialysis, the protein samples were centrifuged 20 min at 95000*g*, concentrated to 3−4 mg/mL with a Centriprep 30 concentrator (Amicon), aliquoted, and flash-frozen in liquid nitrogen for storage at −80 °C. The yield of pure MBP−VanX protein obtained from a 1 L culture of induced *E. coli* BL21(DE3) cells was ∼40 mg.

Thrombin Cleavage of MBP−VanX and Final VanX Purification. MBP was removed from MBP−VanX and the mutant fusion proteins by thrombin proteolysis. To a 3−4 mg/mL solution of MBP−VanX fusion in buffer C was added $CaCl_2$ to a final concentration of 2.5 mM. Restriction-grade thrombin was added (3 units/mg of MBP−VanX fusion protein), and the mixture was incubated at 25 °C for 6 h. Based on SDS−PAGE analysis, over 98% of the fusion proteins were cleaved at this time (data not shown). Under these conditions, mutant E181A partially precipitated after 6 h. Dilution of this fusion protein to a concentration of 2.0 mg/mL prior to treatment with 3 units of thrombin/mg of protein avoided this problem. The cleavage mixture was applied in batches (12 mg of total protein) onto a Resource Q anion exchange column (6 mL, Pharmacia) previously equilibrated with buffer D (20 mM Tris-HCl, pH 8.0) containing 25 mM NaCl at a flow rate of 2 mL/min. Recombinant VanX eluted with a linear gradient of 0.09−0.32 M NaCl in buffer D over 80 mL. During loading, the ionic strength of buffer C caused most of the MBP to elute directly, while VanX was tightly retained on the Resource Q column. VanX eluted in a broad band over 150−225 mM NaCl and was separable from the remaining MBP and thrombin (data not shown). The double mutant C78S/C157S was purified by three passes over Resource Q with a more shallow gradient (0.09−0.32 M NaCl over 125 mL). Fractions (5 mL each) containing pure VanX were pooled, concentrated to 1−2.0 mg/mL with a Centriprep 10 concentrator, aliquoted, and flash-frozen in liquid nitrogen for storage at −80 °C. Protein purity was assessed by SDS−PAGE (Figure 2).

Protein Quantitation and SDS−Polyacrylamide Gel Electrophoresis. Protein concentration during purification and for thrombin cleavage was determined by the Bradford assay (Bradford, 1976) using dye concentrate reagent from Bio-Rad with bovine serum albumin as the standard. The concentration of pure protein was measured by the absorbance at 280 nm according to the method of von Hippel (Gill & von Hippel, 1989) and corrected by amino acid analysis. Proteins were separated by SDS−PAGE using a discontinuous Tris/glycine buffer (Laemmli, 1970) with 12% acrylamide resolving gels and 5% acrylamide stacking gels containing 0.1% SDS.

Circular Dichroic Spectroscopy. Circular dichroism (CD) spectra were recorded with an AVIV Model 62DS CD spectrophotometer (Lakewood, NJ). The CD spectrometer was calibrated prior to measurements with an aqueous solution of (+)-D-10-camphorsulfonic acid (1 mg/mL). The ellipticity, θ_{obs} (λ, 25 °C), of a solution of protein (3−6 μM) in 10 mM phosphate buffer (pH 7.5) was measured at integral values of wavelength (λ) over the range 190−260 nm using an averaging time of 4 s. The CD data are reported as mean residue ellipticity ([θ], in deg cm^2 dmol^{-1}), as calculated by the eq:

$$[\theta]_{(\lambda,T)} = \theta_{obs(\lambda,T)}/10(cdn)$$

where $\theta_{obs(\lambda,T)}$ is the observed ellipticity (in degrees) at a given wavelength and temperature *T*, *c* is the protein concentration (in mol/L), *d* is the optical path length (in cm), and *n* is the number of residues in the protein (205 residues for thrombin-cleaved VanX and mutants).

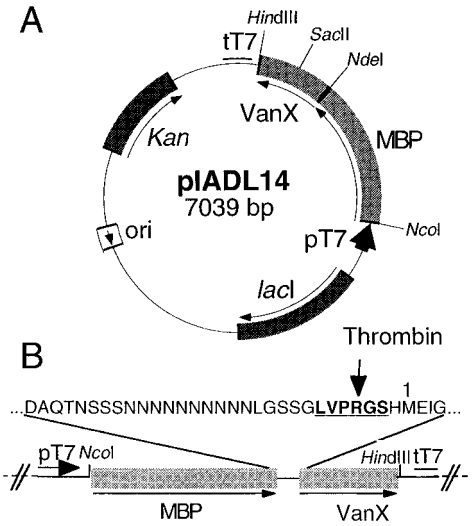

FIGURE 1: Expression vector pIADL14 constructed for expression of the gene encoding the MBP−VanX fusion protein. (A) The construction of the expression vector is described under Experimental Procedures. Genes are shown by differential shading, and the orientations of genes and promoter are indicated with arrows. Kan, kanamycin resistance gene; lacI, *lacI* gene; MBP, *malE* gene encoding the maltose binding protein; ori, origin of ColE1 plasmid replication; pT7, T7 promoter; tT7, T7 terminator; VanX, *vanX* gene. (B) Details of the MBP−VanX fusion junction depicting the serine/asparagine-rich linker and the thrombin cleavage recognition sequence (LVPRGS). Thrombin proteolysis occurs between Arg^{-4} and Gly^{-3} to liberate VanX with an N-terminal tripeptide, Gly-Ser-His, preceding Met^{1} of the wild-type VanX sequence.

Enzyme Activity. Wild-type and mutant enzyme activity was measured in 50 mM HEPES (pH 8.0) with 10 mM D-Ala-D-Ala as substrate at 37 °C according to published procedures (Wu *et al.*, 1995) using the modified cadmium−ninhydrin assay method, which detects the production of free D-Ala (Doi *et al.*, 1981).

ICP−Metals Analysis. Adventitious metals were removed from buffers, dialysis tubing and Slidealyzer dialysis cassettes (Pierce), pipet tips, glassware, and Centriprep 10 concentrators according to published procedures (Auld, 1988). MilliQ water and Chelex-treated buffers were determined to be metal-free by inductively-coupled plasma (ICP) atomic absorption analysis. For quantitation of metals, a solution of MBP−VanX fusion protein (typically 3−5 mg/mL) was dialyzed against six changes of metal-free buffer for 3 h each at a sample/buffer ratio of 1/1000 (v/v), with Chelex resin (10 g/L) included in the buffer reservoir. Samples were subsequently transferred to metal-free Eppendorf tubes, flash-frozen, and analyzed for metal content at the University of Georgia Chemical Analysis Laboratory (Athens, GA). Detection limits for zinc were determined to be <1 ppb.

RESULTS

Overproduction, Purification, and Cleavage of MBP−VanX Fusions. We report here the construction, purification, and assay of 15 mutants of VanX, involving the mutation of 2 cysteine, 5 histidine, 2 aspartate, and 2 glutamate residues to search for loss of function, which might identify residues that could coordinate to zinc and/or participate in D-,D-dipeptide hydrolysis. In general, the strategy was to express the mutants as MBP−VanX fusion proteins from plasmid pIADL14 (Figure 1) and to purify the proteins by affinity chromatography (Figure 2). This fusion protein strategy was adopted because VanX exhibits a severe propensity for aggregation and "spreading" over large regions of chromatographic gradients, making purification and concentration particularly tedious. MBP−VanX overproduced in media containing 200 μM $ZnSO_4$ was as active as VanX, having a catalytic efficiency ratio (k_{cat}/K_M, Table 2) of 50 s^{-1} mM^{-1}, which was similar to the value of 60 s^{-1} mM^{-1} reported previously for wild type (Wu & Walsh, 1995). Removal of the MBP by thrombin proteolysis and anion exchange chromatography (Figure 2) produced no

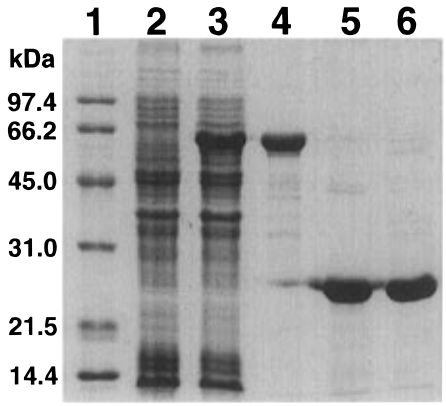

FIGURE 2: Overproduction and purification of VanX. *E. coli* BL21-(DE3) cells were transformed with pIADL14, grown, and induced with IPTG as described under Experimental Procedures. The recombinant MBP−VanX fusion was purified on an amylose column and subjected to thrombin cleavage, and VanX was further purified by anion exchange chromatography. Protein samples were analyzed for purity by SDS−PAGE with Coomassie Blue staining at each stage of the procedure. Lane 1, molecular mass markers (phosphorylase B, 97.4 kDa; serum albumin, 66.2 kDa; ovalbumin, 45.0 kDa; carbonic anhydrase, 31.0 kDa; trypsin inhibitor, 21.5 kDa; lysozyme, 14.4 kDa); lane 2, *E. coli* cells transformed with pIADL14 (before induction); lane 3, clarified lysate of induced cells transformed with pIADL14; lane 4, MBP−VanX protein eluted from the amylose column; lane 5, VanX protein eluted from the anion exchange column; lane 6, VanX protein sample prepared from cells transformed with pZW011 plasmid and purified according to the method of Wu *et al*. (1995).

Table 2: Kinetic Parameters, Zinc Content, and Activity of Purified MBP−VanX Fusion Proteins[a]

protein	k_{cat}[b] (s^{-1})	K_M (mM)	k_{cat}/K_M (s^{-1} mM^{-1})	mol % zinc content[c]	activity
wild type	125.0	2.5	50.0	87.0	active
H13A	83.0	2.1	39.5	91.7	active
H116A	$\leq 5 \times 10^{-3}$	nd[e]	$\leq 10^{-3}$	7.9	inactive
D123A	$\leq 5 \times 10^{-3}$	nd	$\leq 10^{-3}$	≤ 0.04[d]	inactive
E181A	$\leq 5 \times 10^{-3}$	nd	$\leq 10^{-3}$	78.2	inactive
H184A	$\leq 5 \times 10^{-3}$	nd	$\leq 10^{-3}$	0.92	inactive
H116A/H184A	$\leq 5 \times 10^{-3}$	nd	$\leq 10^{-3}$	2.5	inactive
D145A/E146A	20.2	3.7	5.46	89.0	active
H149A/H150A	9.07	2.4	3.78	85.1	active
C78S/C157S	54.1	1.8	30.1	77.5	active

[a] MBP−VanX samples were prepared from cells grown in LB media supplemented with 200 μM $ZnSO_4$. [b] Dipeptidase activity was assayed by measuring the production of D-Ala using the modified cadmium−ninhydrin method (Experimental Procedures). Kinetic parameter values reported are the averages of three determinations. [c] Protein samples for metal analysis were prepared as described under Experimental Procedures. Percentage values reported for moles of zinc/moles of protein are the average of two determinations. [d] Detection limit for inductively-couple plasma analysis of zinc was 1 ppb. Protein concentrations were determined from the corrected absorbance at 280 nm in 6 M guanidine hydrochloride/10 mM phosphate, pH 6.5. [e] Not determined.

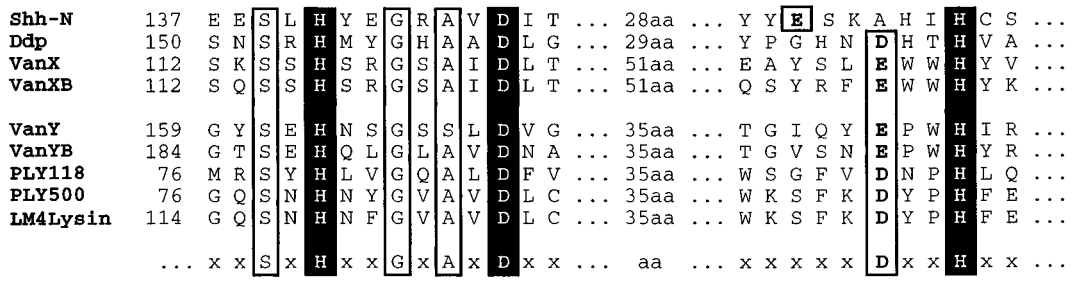

FIGURE 3: Sequence alignment of the zinc binding domain of murine Shh-N, *S. albus* G Ddp, and VanX to homologous regions in putative zinc hydrolases from vancomycin-resistant *Enterococci* (VanXB, VanY, VanYB) and from bacteriophage endolysins (Ply118, Ply500, CPL2438) (see text). Conserved residues among the nine proteins are boxed. Denoted by white letters are the histidine, aspartate, and histidine ligands to zinc found in Shh-N, Ddp, and VanX and predicted zinc binding ligands in the remaining proteins. The glutamate/aspartate catalytic base found in Shh-N, Ddp, and VanX and likely candidates for the other hydrolases are boxed and in boldface type.

significant change in either activity or kinetic parameters of VanX, thereby allowing initial evaluation of mutant enzymes as the MBP fusion constructs. As expected, MBP−VanX contained near-stoichiometric levels of zinc (87.0% mol of zinc/mol of protein).

A complicating factor in VanX production was the rapid loss of the ampicillin-resistant pZW011 plasmid under normal growth conditions. The pET28b(+)-based plasmid encoding kanamycin resistance was subsequently chosen for the MBP−VanX fusions (Figure 1), as kanamycin is more chemically stable than ampicillin in the cell inoculum and the kanamycin gene is in the opposite orientation from the T7 promoter. Probably due to its efficient D-Ala-D-Ala dipeptidase activity, VanX was extremely toxic to its *E. coli* host, routinely causing cell lysis after 90 min of induction. This problem was avoided by limiting the induction time to 75 min or less, and by inducing MBP−VanX expression near cell saturation. Lastly, induction at 37 °C yielded MBP−VanX mostly isolated in the cell debris after centrifugation (>80%), implying inclusion body formation as a result of high levels of gene expression (Williams *et al.*, 1982). Lowering the induction temperature to 30 °C produced completely soluble MBP−VanX protein as judged by SDS−PAGE analysis (data not shown).

Characterization of MBP−VanX Mutants. The assay results of various MBP−VanX mutants are shown in Table 2. Neither of the two cysteine residues, Cys78 and Cys157, is required for catalytic activity or zinc coordination as evidenced by the retention of the catalytic efficiency and the zinc content of the C78S/C157S double mutant (Table 2). The C78S/C157S double mutant shared kinetic parameters similar to wild-type VanX, with only slightly lower zinc content (Table 2).

There are five histidine residues in VanX (His13, His116, His149, His150, and His184). All five single His to Ala mutants were overproduced as the MBP fusions, purified to homogeneity, and assayed (Table 2). Three single histidine mutants retained robust activity equivalent to wild type (H13A, Table 2; H149A, H150A, data not shown). The H149A/H150A double mutant was also active, although k_{cat} was 11-fold lower than wild type, arguing against substitution of one adjacent histidine for the other in a zinc coordination sphere. Two His to Ala mutants (H116A and H184A) lacked any detectable activity even at 400-fold greater enzyme concentrations than wild type. In comparison to wild-type MBP−VanX with 87.0% mol of zinc/mol of of VanX monomer, the zinc content of the H116A and H184A mutants was reduced to 7.9% and 0.92% mol of zinc/mol of protein, respectively. In contrast, the H13A mutant and H149A/H150A double mutant prepared retained 91.7% and 85.1% mol of zinc/mol of protein, respectively, arguing against their involvement in zinc binding (Table 2). The double H116A/H184A mutant was also prepared. As observed with the single mutants, the double mutant was inactive and contained only 2.5% mol of zinc/mol of protein. These results suggest that His116 and His184 are zinc ligands.

There are 16 glutamate and 12 aspartate residues in VanX, making a systematic mutagenesis approach much more difficult to execute. However, we had noted with interest the publication of an X-ray structure of the 19 kDa N-terminal domain of murine Shh-N, an important morphogenic signaling protein in vertebrate development (Perrimon, 1995; Concordet & Ingham, 1995), and the unanticipated finding of zinc in Shh-N (Tanaka-Hall *et al.*, 1995). The metal ion was coordinated to two histidine and one aspartate residues and a water molecule, in an architectural array strikingly similar to the *B. thermoproteolyticus* zinc protease thermolysin (Holden & Matthews, 1988). Although the architectural arrays are similar, the zinc ligands in murine Shh-N (His141, Asp148, and His183) do not present a consensus sequence with the corresponding ligands in thermolysin (His142, His146, and Glu166). However, we had observed that the $\underline{H}_{116}$SRGSAI$\underline{D}_{123}$ sequence in VanX (Figure 3) mimics the seven residue spacing in murine Shh-N ($\underline{H}_{141}$YEGRAV$\underline{D}_{148}$) and fits a consensus of SxHxxGxAxD in which histidine and aspartate are the zinc ligands in Shh-N. We, therefore, mutated Asp123 to alanine. The resulting VanX mutant was inactive (k_{cat} less than 0.05% of wild type) and retained <1% of zinc (detection limits <1 ppb), strongly implicating this β-carboxylate side chain as a zinc ligand. As a control, Asp145 and Glu146 were each mutated to alanine and found to retain full activity (data not shown). Furthermore, the double D145A/E146A mutant was constructed and was also found to be active (k_{cat} was 6-fold lower than wild type). This construct retained 89.0% mol of zinc/mol of protein, further arguing for the role of Asp123 as a zinc coordinating residue (Table 2).

A recent review by Murzin (1996) called attention to a common protein fold and reported identical coordination of zinc in murine Shh-N and in *S. albus* G Ddp. The X-ray structure of the *S. albus* Ddp at 2.5 Å, reported in 1982, assigned His152, His193, and His196 as ligands for zinc with two aspartate residues in proximity (Asp161 and Asp194), although the amino acid sequence had not been fully reported at that time. The 212 amino acid sequence of Ddp was subsequently determined by chemical methods (Joris *et al.*,

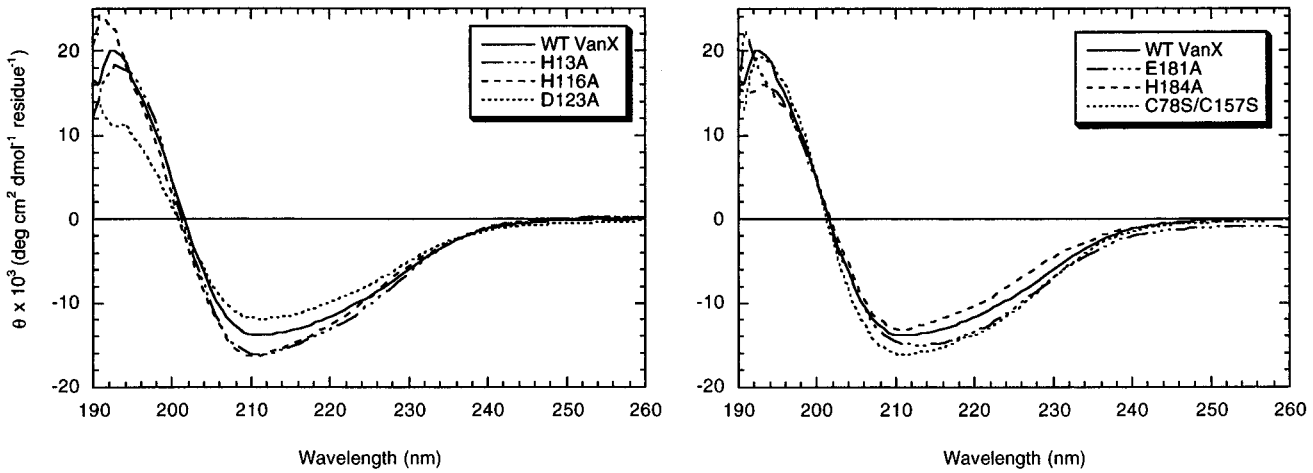

FIGURE 4: Circular dichroism spectra for seven thrombin-cleaved VanX proteins, three which are catalytically active (wild type, H13A, and C78S/C157S) and four of which are inactive (H116A, D123A, E181A, and H184A).

1983) and later revised to 213 amino acids based on the derived DNA sequence from the cloned gene which reflected the omission of a residue (Duez *et al.*, 1990). Therefore, the numbering scheme used by Dideberg *et al.* (1982) which identified His residues at 153, 193, and 196 should be increased by one to reflect the correct residue position (His residues at 154, 194, and 197). As shown in Figure 3, use of the SxHxxGxAxD consensus sequence from VanX and Shh-N in the Clustal W multiple sequence alignment program (Thompson *et al.*, 1994) suggests that *S. albus* G Ddp residues 152−161 fit this pattern exactly with the Asp161 in Ddp corresponding to Asp123 in VanX and likewise Asp148 coordinating zinc in murine Shh-N. Figure 1 of Murzin's review shows the His, His, Asp metal ligand arrangement for *S. albus* G Ddp (see Discussion).

Search for a Catalytic Base. The X-ray structures of *B. thermoproteolyticus* thermolysin and murine Shh-N display a conserved glutamate residue adjacent to the coordinated zinc, hydrogen-bonded to the active site water molecule, which in turn is the fourth ligand to zinc (Tanaka-Hall *et al.*, 1995). In thermolysin, the corresponding acid residue is Glu143, and it has been assigned the role of catalytic base, to activate the water molecule for nucleophilic attack on bound substrate, and initiate peptide bond cleavage. In *S. albus* G Ddp, there is an aspartate residue (Asp194) three residues upstream of the zinc-coordinating His197, which is proposed to play an identical role (Dideberg *et al.*, 1982; Ghuysen, 1988). By analogy, Glu181, three residues from His184 in VanX, seemed a likely candidate for a catalytic base. Thus, the E181A VanX mutant was constructed, purified, and assayed both for catalytic activity and for zinc content. There was no detectable D-Ala-D-Ala dipeptidase activity as noted in Table 2, where 0.05% of wild-type enzyme could have been detected. Meanwhile 78.2% mol of zinc/mol of protein was retained, consistent with Glu181 functioning as a catalytic base and not as a structural ligand for zinc.

Circular Dichroism. CD spectra of the thrombin-cleaved native enzyme and six mutants were obtained in order to delineate whether mutant inactivation and zinc loss were due to gross conformational changes. Shown in Figure 4 are the CD spectra of seven proteins recorded at pH 7.5 in 10 mM phosphate buffer, three of which are catalytically active (wild-type VanX, H13A, and C78S/C157S) and four mutants which exhibit no activity (H116A, D123A, E181A, and H184A). CD data have been corrected for concentration and subjected to 7-point smoothing, and are reported as the mean residue ellipticity. All proteins exhibited similar spectra with minima near 210 nm and maxima near 194 nm, implying that the inactive mutants exhibit a fold similar to wild-type VanX and that mutational inactivation does not perturb the overall conformation but affects only the active site architecture.

DISCUSSION

VanX is of interest for structure−function analysis as a D-Ala-D-Ala dipeptidase because it is a potential target enzyme for reversal of vancomycin resistance in vancomycin-resistant enterococcal pathogens. We have previously reported both zinc dependence for dipeptide hydrolysis by VanX (Wu *et al.*, 1995) and its potent inhibition by slow binding phosphinate dipeptide analogues, which mimic the tetrahedral adduct that would arise by the direct attack of zinc-coordinated water on D-Ala-D-Ala (Wu & Walsh, 1995). Herein, the zinc content and catalytic activity of both wild type and several mutant forms of VanX have been assessed.

In this study, a mutagenesis approach was undertaken to identify residues in VanX that may be ligands for zinc, and to gain insight into residues that could define the active site. Since initial homology searches failed to reveal any obvious zinc ligand signature patterns, each of the two cysteine residues, Cys78 and Cys157, were mutated, given the known high affinity of thiols as zinc ligands. Retention of activity and zinc content by these mutants ruled out any role for these residues in either catalytic activity or zinc binding. We subsequently investigated the five histidine residues in VanX and observed three His to Ala mutants that left catalytic activity unimpaired. However, the H116A and H184A mutants lost all detectable activity and purified with 7.9% and 0.92% of the stoichiometric quantity of zinc, respectively, suggesting that these imidazole side chains are two of the four anticipated zinc ligands in VanX.

The publication of the X-ray structure of murine Shh-N with zinc coordinated to His141, Asp148, His183, and a water molecule and with essentially identical ligands and geometry as observed in the protease thermolysin by Tanaka-Hall *et al.* (1995) focused our attention on the possibility of a carboxylate side chain as a potential third ligand in VanX.

Scheme 1 [a]

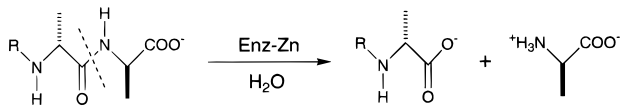

[a] R = H: VanX substrate. R = acyl: Ddp substrate.

Given a total of 28 aspartate and glutamate residues in VanX, we first searched for any short sequence motif that could serve as a guide for mutational analysis and noted that the sequence SxHxxGxAxD was conserved in both VanX and Shh-N. Significantly, His116 in the consensus sequence was one of the inactivating mutations in VanX, and the corresponding His141 in murine Shh-N was a known zinc ligand. Furthermore, Asp148 in Shh-N was also a zinc ligand and, based on the consensus sequence, corresponded to Asp123 in VanX. Therefore, we constructed the D123A VanX mutant, which was indeed observed to be both inactive and zinc-deficient, results consistent with a role of this residue as a zinc ligand in VanX.

A recent review by Murzin (1996) drew our attention to the *S. albus* G Ddp as a zinc-dependent *N*-acyl-D-Ala-D-Ala carboxypeptidase which exhibits mechanistic analogy to VanX and shares an identical zinc coordination geometry and mechanism for catalytic water activation (Scheme 1). The initial X-ray structure report at 2.5 Å resolution of the *S. albus* G Ddp (Dideberg *et al.*, 1982) identified three histidine residues (His154, His195, and His197) as zinc ligands, but the primary sequence was not reported at that time. Comprising 213 residues (Duez *et al.*, 1990), Ddp is similar in length to VanX (202 residues), the latter also exhibiting comparable His content (5 histidines). The five histidine residues of *S. albus* G Ddp are located at positions 154, 158, 192, 195, and 197. Homology searches with the consensus SxHxxGxAxD pattern located a match in Ddp (Figure 3), with conservation of an aspartate residue (Asp161) seven residues away from His154, and suggested that the zinc ligand site for Ddp comprised His154, Asp161, and His197 (from Clustal W sequence aligment analysis) as shown in Figure 3. Murzin (1996) has also concluded that two histidine and one aspartate residues rather than three histidine residues comprise the ligands to zinc in Ddp. In confirmation of this analysis, Ghuysen, in a chapter published in 1988, citing a Ph.D. thesis (J. D. Wery, University of Liege, 1987) describes Wery's 1.5 Å resolution X-ray structure of *S. albus* G Ddp which indeed reassigned His154, Asp161, and His197 as the zinc ligands. Further searches with the 10 amino acid sequence string reveal an equivalent zinc site in VanY, an *N*-acyl-D-Ala-D-Ala carboxypeptidase, previously described in vancomycin-resistant *Enterococci* (Wright *et al.*, 1992; Arthur *et al.*, 1994). The 10 amino acid sequence string also identifies this motif (Figure 3) in the PLY118, PLY500, and CPL2438 endolysins encoded by bacteriophages that infect *Listeria* strains (Loessner *et al.*, 1995; Zink *et al.*, 1995). While it remains to be determined whether these proteins are zinc-dependent enzymes, there is the intriguing correlation that PLY118 and PLY500 (and probably CPL2438) are L-alanyl-D-glutamyl peptidases that function, in analogy to the *S. albus* Ddp, to cleave bacterial cell peptidoglycans. The L,D- or D,D-peptide cleaving reactions catalyzed by Ddp, the bacteriophage endolysins, and VanX are so similar as to suggest that there will be common patterns of peptide substrate recognition and architectural similarity between these proteins. The lack of apparent primary sequence homology implies that one must await the three-dimensional structure of VanX for a full evaluation. Secondary structure predictions do not allow a clear mapping of α-helix and *β*-sheet secondary structure from VanX onto the two-domain Ddp (Murzin, 1996; Dideberg *et al.*, 1982) although high helical content in the 10 amino acid SxHxxGxAxD motif is predicted (data not shown). Unlike Ddp, VanX will not bind or hydrolyze N-acetylated D-Ala-D-Ala dipeptides, requiring instead the presence of a free α-amino group in the D,D-dipeptide. It may be of interest to assess whether Ddp will hydrolyze *N*-acyl-D-Ala-D-lactate given the chemoselectivity of VanX to hydrolyze the dipeptide but not the depsipeptide substrate. The determination of a likely set of zinc ligands in VanX and homology to the revised zinc ligand set for Ddp provide insights into the active site catalytic architecture for D,D-dipeptide recognition and hydrolysis, which may reflect convergent evolution of VanX and Ddp, and may make Ddp a good model for structure-based leads of VanX inhibitors. Lastly, in both Shh-N and thermolysin (and most probably Ddp, VanX, VanY, and other members of this zinc-dependent peptide bond-hydrolyzing enzyme family), a water molecule is the fourth ligand to zinc, and its nucleophilicity is enhanced by hydrogen bonding to a carboxylate residue (e.g., Glu143 in *B. thermoproteolyticus* thermolysin) acting as a general base. By homology, candidates for this function in *S. albus* G Ddp and VanX are Asp194 and Glu181, respectively, validated experimentally herein for VanX by analysis of the E181A mutant.

We therefore suggest the following mechanism for D-Ala-D-Ala cleavage (Scheme 2), involving substrate coordination to zinc, followed by generation of a tetrahedral adduct (possibly with pentacoordinated zinc as postulated for thermolysin; Izquierdo-Martin & Stein, 1992). This assessment of the mechanism may serve as a useful guide for VanX inhibitor design and evaluation as well as for analyses of dipeptide versus depsipeptide recognition.

ACKNOWLEDGMENT

We are grateful to Ms. Rebecca Auxier of the University of Georgia Chemical Analysis Laboratory for ICP-metal

Scheme 2

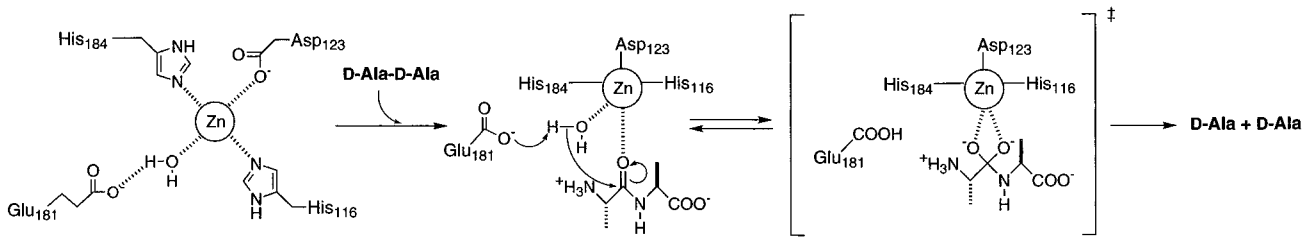

analyses, Mr. Ivar Jansen of the Howard Hughes Biopolymer facility for amino acid analyses, and Professors Don Wiley and Steve Harrison of Harvard University for access to their CD spectrophotometer. We thank Dr. Stewart Fisher, Dr. Zhen Wu, Dr. Ranabir Sinha Roy, Dr. Wolfgang Maret, Dr. David Auld, Dr. Bert Vallee, and members of the Walsh laboratory for helpful and insightful discussions.

REFERENCES

Arthur, M., & Courvalin, P. (1993) *Antimicrob. Agents Chemother. 37*, 1563−1571.
Arthur, M., Molinas, C., Depardieu, F., & Courvalin, P. (1993) *J. Bacteriol. 175*, 117−127.
Arthur, M., Depardieu, F., Snaith, H. A., Reynolds, P. E., & Courvalin, P. (1994) *Antimicrob. Agents Chemother. 38*, 1899−1903.
Auld, D. S. (1988) *Methods Enzymol. 158*, 71−79.
Barna, J. C. J., & Williams, D. H. (1984) *Annu. Rev. Microbiol. 38*, 339−357.
Billot-Klein, D., Gutmann, L., Sable, S., Guittet, E., & Heijenoort, J. (1994) *J. Bacteriol. 176*, 2398−2405.
Bradford, M. M. (1976) *Anal. Biochem. 72*, 248−254.
Bugg, T. D. H., Dutka-Malen, S., Arthur, M., Courvalin, P., & Walsh, C. T. (1991a) *Biochemistry 30*, 2017−2021.
Bugg, T. D. H., Wright, G. D., Dutka-Malen, S., Arthur, M., Courvalin, P., & Walsh, C. T. (1991b) *Biochemistry 30*, 10408−10415.
Concordet, P.-P., & Ingham, P. (1995) *Nature 375*, 279−280.
Dideberg, O., Charlier, P., Dive, G., Joris, B., Frere, J. M., & Ghuysen, J. M. (1982) *Nature 299*, 469−470.
Doi, E., Shibata, D., & Matoba, T. (1981) *Anal. Biochem. 118*, 173−184.
Duez, C., Lakaye, B., Houba, S., Dusart, J., & Ghuysen, J. M. (1990) *FEMS Microbiol. Lett. 71*, 215−220.
Ghuysen, J. M. (1988) in *Antibiotic Inhibition of Bacterial Cell Surface Assembly and Function* (Actor *et al.*, Eds.) pp 268−284, American Society for Microbiology, Washington, DC.
Gill, S. C., & von Hippel, P. H. (1989) *Anal. Biochem. 182*, 319−326.
Holden, H. M., & Matthews, B. W. (1988) *J. Biol. Chem. 263*, 3256−3265.
Handwerger, S., Pucci, M. J., Volk, K., Lui, J., & Lee, M. (1994) *J. Bacteriol. 176*, 260−264.
Ho, S. N., Hunt, H. D., Horton, R. M., Pullen, J. K., & Pease, L. R. (1989) *Gene 77*, 51−59.
Izquierdo-Martin, M., & Stein, R. L. (1992) *J. Am. Chem. Soc. 114*, 325−331.
Joris, B., Van Beeuman, J., Casagrande, F., Gerday, C., Frere, J. M., & Ghuysen, J. M. (1983) *Eur. J. Biochem. 130*, 53−69.
Laemmli, U. K. (1970) *Nature 227*, 680−685.
Lessard, I. A. D., & Perham, R. N. (1994) *J. Biol. Chem. 269*, 10378−10383.
Loessner, M. J., Wendlinger, G., & Scherer, S. (1995) *Mol. Microbiol. 16*, 1231−1241.
Messer, J., & Reynolds, P. E. (1992) *FEMS Microbiol. Lett. 94*, 195−200.
Murzin, A. G. (1996) *Curr. Opin. Struct. Biol. 6*, 386−394.
Park, I.-S., & Walsh, C. T. (1997) *J. Biol. Chem. 272*, 9210−9214.
Perrimon, N. (1995) *Cell 80*, 517−520.
Reynolds, P. E. (1989) *Eur. J. Microb. Infect. Dis. 8*, 943−950.
Reynolds, P. E., Depardieu, F., Dutka-Malen, S., Arthur, M., & Courvalin, P. (1994) *Mol. Microbiol. 13*, 1065−1070.
Saiki, R. K., Scharf, S., Faloona, F., Mullis, K., Horn, G. T., Erlich, H. A., & Arnheim, N. (1985) *Science 230*, 1350−1354.
Saiki, R. K., Gelfland, D. H., Stoffel, S., Scharf, S., Higuchi, R., Faloona, F., Horn, G. T., Mullis, K., & Erlich, H. A. (1988) *Science 239*, 487−491.
Sambrook, J., Fritsch, E. F., & Maniatis, T. (1989) *Molecular Cloning: A Laboratory Manual*, 2nd ed., Cold Spring Harbor Laboratory, Cold Spring Harbor, NY.
Swartz, M. N. (1994) *Proc. Natl. Acad. Sci. U.S.A. 91*, 2420−2427.
Tanaka-Hall, T. M., Porter, J. A., Beachy, P. A., & Leahy, D. J. (1995) *Nature 378*, 212−216.
Thompson, J. D., Higgins, D. G., & Gibson, T. J. (1994) *Nucleic Acids. Res. 22*, 4673−4680.
Vallee, B. L., & Auld, D. S. (1990) *Biochemistry 29*, 5647−5659.
Walsh, C. T. (1993) *Science 261*, 308−309.
Walsh, C. T., Fisher, S. L., Park, I.-S., Prahalad, M., & Wu, Z. (1996) *Chem. Biol. 3*, 21−28.
Williams, D. C., Frank, R. M. V., Muth, W. L., & Burnett, J. P. (1982) *Science 215*, 687−689.
Wright, G. D., & Walsh, C. T. (1992) *Acc. Chem. Res. 25*, 468−473.
Wright, G. D., Molinas, C., Arthur, M., Corvalin, P., & Walsh, C. T. (1992) *Antimicrob. Agents Chemother. 36*, 1514−1518.
Wright, G. D., Holman, T. R., & Walsh, C. T. (1993) *Biochemistry 32*, 5057−5063.
Wu, Z., & Walsh, C. T. (1995) *Proc. Natl. Acad. Sci. U.S.A. 92*, 11603−11607.
Wu, Z., & Walsh, C. T. (1996) *J. Am. Chem. Soc. 118*, 1785−1786.
Wu, Z., Wright, G., & Walsh, C. T. (1995) *Biochemistry 34*, 2455−2463.
Zink, R., Loessner, M. J., & Scherer, S. (1995) *Microbiology 141*, 2577−2584.

BI970543U